Serb. Astron. J. № 177 (2008), 61 - 66
DOI: 10.2298/SAJ0877061C

UDC 524.354–77 : 524.722.3
Original Scientific Paper

RADIO-CONTINUUM STUDY OF THE SUPERNOVA REMNANTS IN THE LARGE MAGELLANIC CLOUD – AN SNR WITH A HIGHLY POLARISED BREAKOUT REGION – SNR J0455–6838

E. J. Crawford[1], M. D. Filipović[1], A. Y. De Horta[1], F. H. Stootman[1] and J. L. Payne[2]

[1] *School of Computing and Mathematics, University of Western Sydney Locked Bag 1797, Penrith South DC, NSW 1797, Australia*

E–mail: *e.crawford@uws.edu.au*

[2] *Centre for Astronomy, James Cook University Townsville, QLD 4811, Australia*

(Received: August 15, 2008; Accepted: August 29, 2008)

SUMMARY: We present the results of new moderate resolution ATCA observations of SNR J0455–6838. We found that this SNR exhibits a mostly typical appearance with rather steep and curved α=–0.81$\pm$0.18 and D=43$\times$31$\pm$1 pc. Regions of high polarisation were detected, including unusually strong ($\sim$70%) region corresponding to the northern breakout. Such a strong polarisation in breakout regions has not been observed in any other SNR.

Key words. ISM: supernova remnants – Magellanic Clouds – Radio Continuum: ISM – Polarization – ISM: individual objects – SNR J0455–6838

1. INTRODUCTION

The Large Magellanic Cloud (LMC), with its low foreground absorption and relative proximity of 50 kpc (Hilditch et al. 2005), offers the ideal laboratory for the study of a complete sample of supernova remnants (SNRs) in great detail. The proximity enables detailed spatial studies of the remnants in the sample, and the accurately known distance allows for analysis of the energetics of each remnant. In addition, the wealth of wide-field multiwavelength data available, from radio maps to optical emission-line images and broad band photometry to global X-ray mosaics, provides information about the contexts and environments in which these remnants are born and evolve.

It is possible to obtain a relatively complete sample of SNRs in the LMC and not only study the global properties of the sample but also study the subclasses in detail (e.g., sorted by X-ray and radio morphology or by progenitor SN type). Toward this goal, we have been identifying new SNRs using combined optical, radio, and X-ray observations. There are over 40 confirmed SNRs in the LMC and another 35-40 candidates (Payne et al. 2008).

Here, we report on radio-continuum observation of a previously known and intriguing SNR, SNR J0455–6838. It was initially classified as an SNR based on observations made by the Mills Cross telescope at the Molonglo Radio Observatory at 408 MHz (Mathewson and Clarke 1973). Further confirmation comes from the Einstein X-Ray survey by Long et al. (1981) (named LHG 2) and Wang et al. (1991) (named W 3). Mathewson et al. (1983) catalogued SNR J0455–6838 as B0455–68.7 based on their optical observations, reporting an estimated size of 217″ × 183″. Filipović et al. (1998) added further confirmation, with a set of radio-continuum observations (with the Parkes telescope) over a wide frequency range. Blair et al. (2006) report no detection at far ultraviolet (FUV) wavelengths. Haberl and Pietsch (1999) (named SNR as HP 915) and Williams et al. (1999) discuss the X-ray properties of the SNR J0455–6838 based on ROSAT observations. Most recently Payne et al. (2008) presented optical spectroscopy of a wide range of LMC SNRs including SNR J0455–6838. They found an enhanced [S II]/H_α ratio of 0.6 typical for SNRs.

2. OBSERVATIONAL DATA

We observed SNR J0455–6838 with the Australia Telescope Compact Array (ATCA) on 6th April 1997, with an array configuration EW375, at wavelengths of 6 and 3 cm (ν=4790 and 8640 MHz). The observations were carried out in the so called "snap-shot" mode, totaling ∼1 hour of integration over a 12 hour period. Source 1934-638 was used for primary calibration and source 0530-727 was used for secondary calibration. The MIRIAD (Sault and Killeen 2006) and KARMA (Gooch 2006) software packages were used for reduction and analysis. More information about observing procedure and other sources observed during this session can be found in Bojičić et al. (2007) and Crawford et al. (2008).

Images were prepared, cleaned and deconvolved using MIRIAD tasks. Baselines formed with the 6th ATCA antenna were excluded, as the other five antennas were arranged in a compact configuration. The 6-cm image (Fig. 1) has a resolution of 26″ and the r.m.s noise is estimated to be 0.2 mJy/beam. Similarly, the 3-cm image (Fig. 2(a)) has a resolution of 26″ and the r.m.s noise is estimated to be 0.3 mJy/beam. The 3-cm image resolution of 26″ was chosen to complement the 6-cm image, and was used in the preparation of Figs. 2 and 3.

3. RESULTS AND DISCUSSION

The remnant has a classical horseshoe morphology centered at RA(J2000)=$4^h55^m45.7^s$, DEC(J2000)=−68°38′52.9″ with a diameter of 215″×156″±5″ (43×31±1 pc), excluding the breakout region to the north. This is reasonably consistent with the optical size reported by Mathewson et al. (1983). The X-ray size of 366″ × 168″ reported by Williams et al. (1999), seems to include the breakout region to the north and, when removed, our diameters are in agreement.

Breakout regions are rarely seen in SNRs, and Williams et al. (1999b) indicated that they may have a significant role in SNR evolution. They report a northern and southern breakout; however, we only detect the northern one.

Flux density measurements were made at 6 cm and 3 cm, resulting in values of 115 mJy and 30 mJy respectively (Table 1), although our data seem to suffer from "short-spacing" effects and some flux may have been missed. Using the 21-cm mosaic image described in Hughes et al. (2007), we made a new measurement of the flux density of SNR J0455–6838, obtaining a value of 289 mJy. A spectral index (defined by $S \propto \nu^\alpha$) was plotted using the flux densities in Table 1 (Fig. 3(b)) and estimated to be α=−0.81±0.18, which is very steep for SNRs (Filipović et al. 1998). The previous spectral index estimate was based solely on single dish data, and was α=−0.43±0.05 (Filipović et al. 1998). As shown in Fig. 3(b), we note that the 3 cm and 6 cm points are low compared to the others, which indicates that a simple model does not accurately describe the data, and that a higher order model is needed. This is not unusual, given that several other SNR's exhibit this "curved" spectra (Filipović et al. 1998). Noting the breakdown of the power law fit at shorter wavelengths, we decomposed the spectral index estimate into two components, one (α_1) between 73 and 13 cm, and the other (α_2) between 13 and 3 cm. The first component, $\alpha_1 = -0.35 \pm 0.08$ is a very good fit and typical for an SNR, whereas the second, $\alpha_2 = -1.52 \pm 0.39$, is a poor fit, and indicates that non-thermal emission can be described by different populations of electrons with different energy indices. Although the low flux at 3 cm (and to a lesser extent at 6 cm) could cause the large deviations, an underestimate of up to ∼50% would still lead to a "curved" spectrum.

From our spectral index map (Fig. 3(a)) one can see a very steep gradient of spectral index, caused by the lower than expected 3-cm flux density. Comparison of our radio-continuum images with ROSAT HRI X-ray images of Williams et al. (1999; Fig. 1v) shows a correlation between radio and X-ray emissions, as X-ray emission may be dominated by non-thermal emission.

Linear polarisation images for each frequency were created using Q and U parameters. While we detect no reliable polarisation at 3-cm, the 6-cm image reveals some very unusually strong linear polarisation. Without reliable polarisation measurements at the shorter wavelength, we could not determine the Faraday rotation.

Table 1. Integrated Flux Density of SNR J0455–6838.

S_I	73 cm	36 cm	21 cm	13 cm	6 cm	3 cm
SNR J0455–6838	410 mJy	380 mJy	289 mJy	229 mJy	115mJy	33 mJy
Reference	Clarke et al. 1976	Mills et al. 1984	This Work	Filipović et al. 1996	This Work	This Work

The mean fractional polarisation at 6-cm was calculated using flux density and polarisation:

$$P = \frac{\sqrt{S_Q^2 + S_U^2}}{S_I} \cdot 100\% \qquad (1)$$

where S_Q, S_U and S_I are integrated intensities for the Q, U and I Stokes parameters. Our estimated peak value is $P \sim 70\%$ in the breakout region, where the total intensity is relatively low. This could be due to the breakout interacting with the interstellar medium. This effect has not been seen before as SNRs with clear breakouts are rare, nor has such strong polarisation been seen, even in strongly polarised SNRs. Along the brightest section of the shell the polarisation is relatively uniform, and quite strong at approximately 20% (Fig. 1), as would be expected from non-thermal SNRs. This relatively high level of polarisation is (theoretically) expected for an SNR with a radio spectrum of less than −0.5 (Rolfs and Wilson 2003).

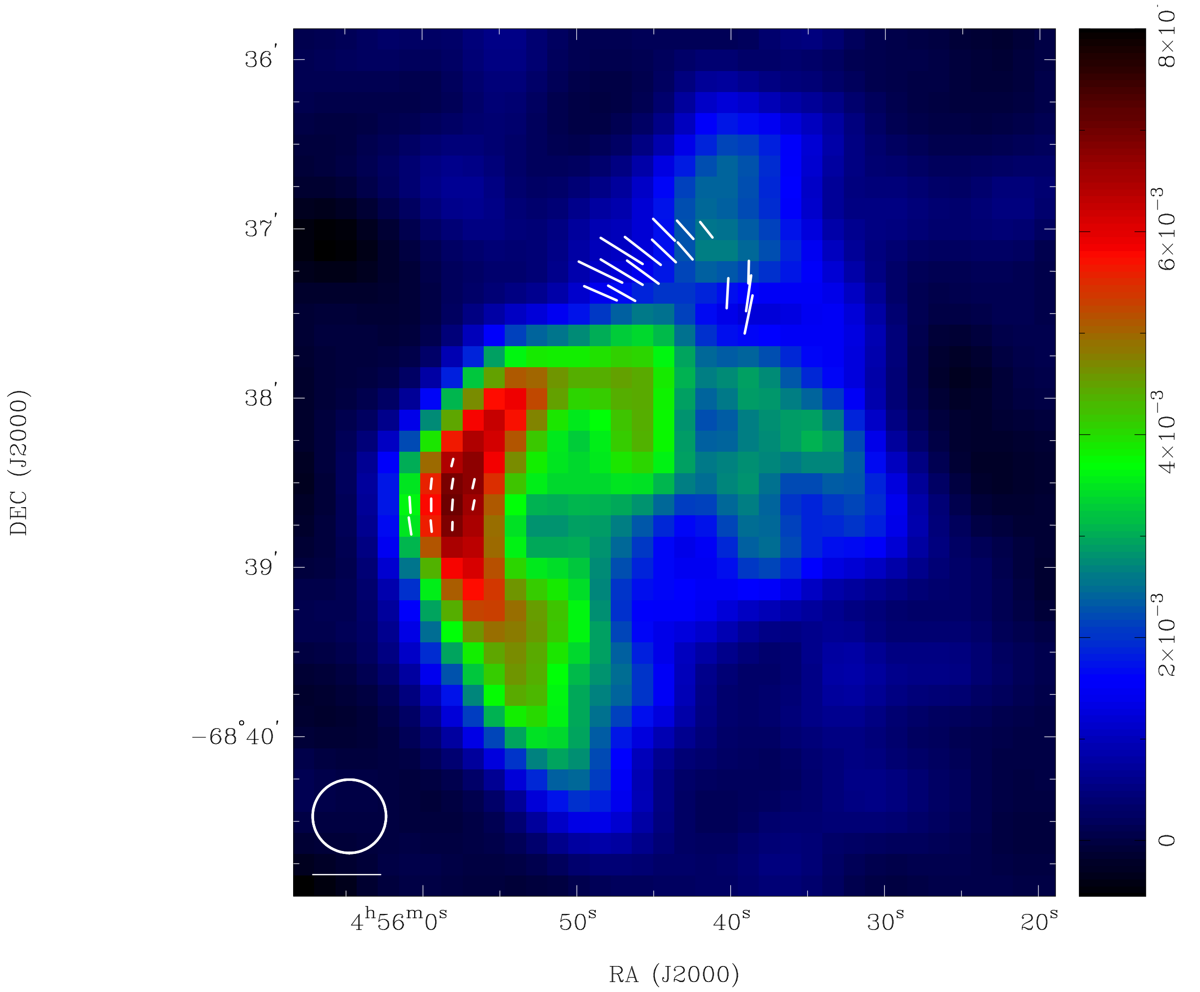

Fig. 1. *ATCA observations of SNR J0455–6838 at 6 cm (4790 MHz) overlaid with fractional polarised intensity. The white circle in the lower left corner represents the synthesised beam of 26″, and the white line below the circle is a polarisation vector of 100%. The sidebar quantifies the pixel map and its units are Jy/beam.*

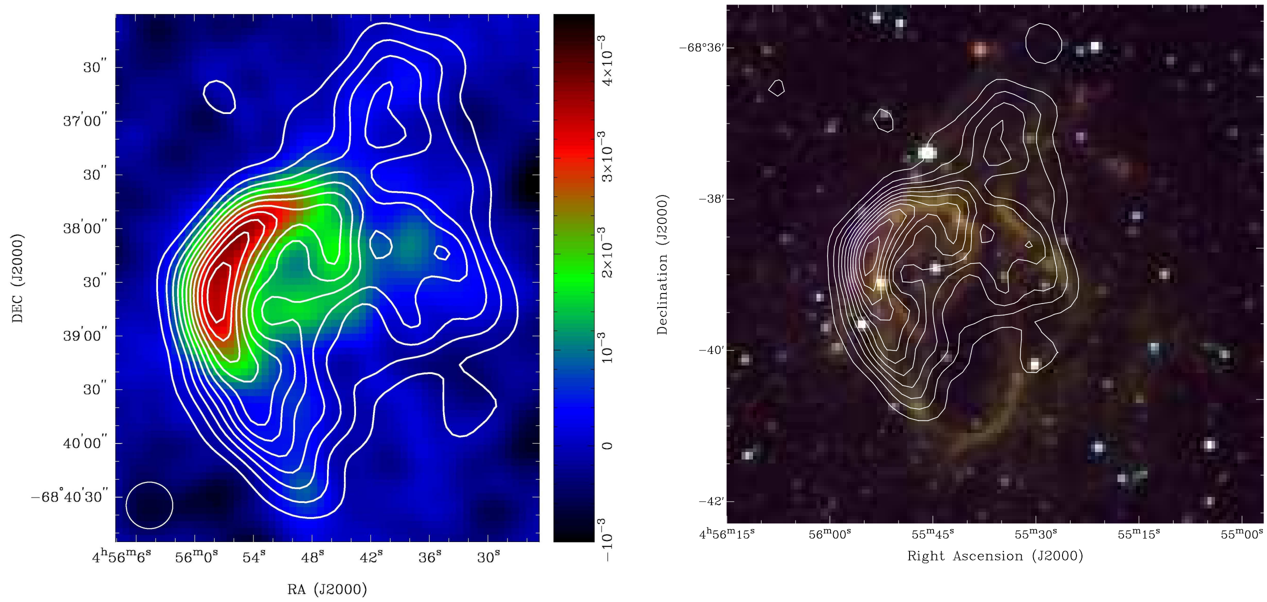

Fig. 2. *(a)ATCA 3-cm observations of SNR J0455–6838, overlaid with 6-cm contours. The white circle in the lower left corner represents the 3 cm (8640 MHz) synthesised beam of 26″. The sidebar quantifies the pixel map and its units are Jy/beam. (b) MCELS composite optical image* (RGB = H_α,[SII],[OIII]) *overlaid with ATCA 6-cm contours. The contours on both images are 3–33σ in 3σ steps.*

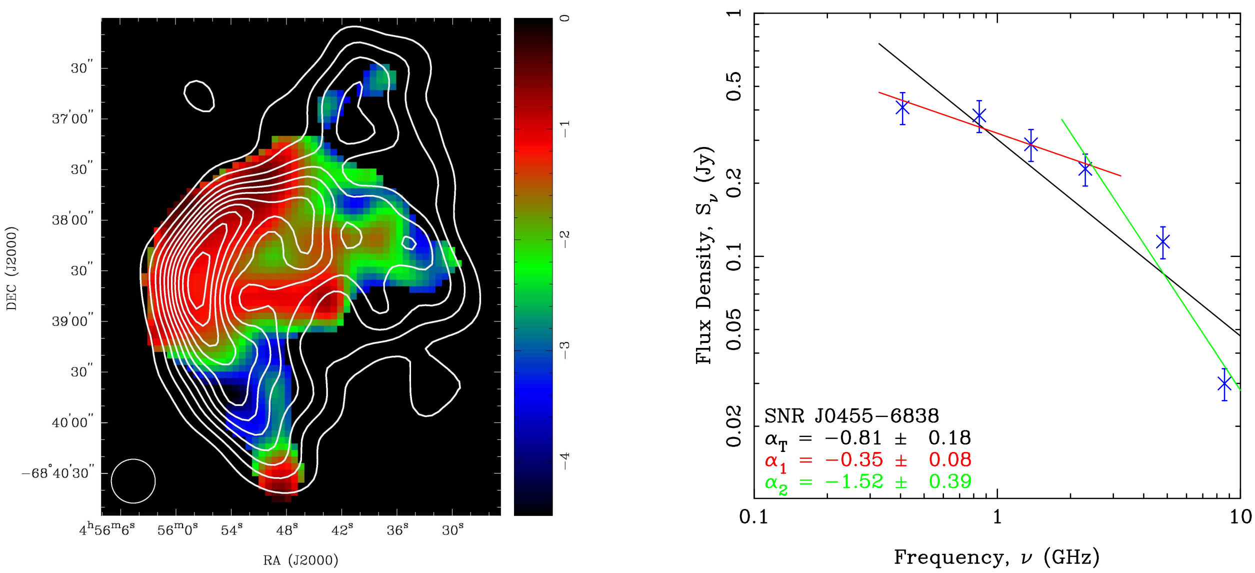

Fig. 3. *(a) Spectral index map of SNR J0455–6838 overlaid with 6 cm (4790 MHz) contours. The contours are the same as in Fig. 2. The white circle in the lower left corner represents the synthesised beam of 26″. The sidebar quantifies the pixel map, representing the spectral index. (b) Radio-continuum Spectrum of SNR J0455–6838.*

4. CONCLUSION

We conducted the highest resolution radio-continuum observations to date of SNR J0455–6838. From these observations we found a diameter of $215'' \times 156'' \pm 5''$, a complex spectral index α=–0.81±0.18 and interesting polarisation features associated with the brightest region of the SNR and the northern breakout region.

Acknowledgements – We used the KARMA software package developed by the ATNF. The Australia Telescope Compact Array is part of the Australia Telescope which is funded by the Commonwealth of Australia for operation as a National Facility managed by CSIRO. We thank the Magellanic Clouds Emission Line Survey (MCELS) team for access to the optical images. We thank the referee for numerous helpful comments that have greatly improved the quality of this paper.

REFERENCES

Blair, W. P., Ghavamian, P., Sankrit, R., Danforth, C. W.: 2006, *Astron. Astrophys. Suppl. Series*, **165**, 480.

Bojičić, I. S., Filipović, M. D., Parker, Q. A., Payne, J. L., Jones, P. A., Reid, W., Kawamura, A., Fukui, Y.: 2007, *Mon. Not. R. Astron. Soc.*, **378**, 1237.

Clarke, J. N., Little, A. G., Mills, B. Y.: 1976, *Aust. J. Phys. Astrophys. Suppl.*, **40**, 1.

Crawford E. J., Filipović, M. D. and Payne, J. L.: 2008, *Serb. Astron. J.*, **176**, 59.

Filipović, M. D., White, G. L., Haynes, R. F., Jones, P. A., Meinert, D., Wielebinski, R., Klein, U.: 1996, *Astron. Astrophys. Suppl. Series*, **120**, 77.

Filipović, M. D., Haynes, R. F., White, G. L., Jones, P. A.: 1998, *Astron. Astrophys. Suppl. Series*, **130**, 421.

Gooch, R.: 2006, Karma Users Manual, ATNF, Sydney.

Haberl, F., Pietsch, W.: 1999, *Astron. Astrophys. Suppl. Series*, **139**, 277.

Hilditch, R. W., Howarth, I. D., Harries, T. J.: 2005, *Mon. Not. R. Astron. Soc.*, **357**, 304.

Hughes, A., Staveley-Smith, L., Kim, S., Wolleben, M., Filipović, M.: 2007, *Mon. Not. R. Astron. Soc.*, **382**, 543.

Long, K. S., Helfand, D. J., Grabelski, D. A.: 1981, *Astrophys. J.*, **248**, 925.

Mathewson, D. S. and Clarke, J. N.: 1973, *Astrophys. J.*, **180**, 725.

Mathewson, D. S., Ford, V. L., Dopita, M. A., Tuohy, I. R., Long, K. S., Helfand, D. J.:1983, *Astron. Astrophys. Suppl. Series*, **51**, 345.

Mills, B. Y., Turtle, A. J., Little, A. G., Durdin, J. M.: 1984, *Aust. J. Phys.*, **37**, 321.

Payne, J. L., White, G. L., Filipović, M. D.: 2008, *Mon. Not. R. Astron. Soc.*, **383**, 1175.

Rolfs, K., Wilson, T.: 2003: "Tools of Radio Astronomy 4ed.", Springer, Berlin.

Sault, R., Killeen, N.: 2006, Miriad Users Guide, ATNF, Sydney.

Wang, Q., Hamilton, T., Helfand, D. J., Wu X.: 1991, *Astrophys. J.*, **374**, 475.

Williams, R. M., Chu, Y.-H., Dickel, J. R., Petre, R., Smith, R. C., Tavarez, M.: 1999, *Astrophys. J. Suppl. Series*, **123**, 467.

Williams, R. M., Chu, Y.-H., Dickel, J. R., Smith, C. R., Milne, D. K. and Winkler, P. F.: 1999b, *Astrophys. J.*, **514**, 798.

РАДИО-КОНТИНУМ СТУДИЈА ОСТАТАКА СУПЕРНОВИХ У ВЕЛИКОМ МАГЕЛАНОВОМ ОБЛАКУ – ОСТАТАК СУПЕРНОВЕ СА ВИСОКО-ПОЛАРИЗОВАНИМ РЕГИОНОМ ПРОБОЈА МАТЕРИЈЕ – SNR J0455–6838

E. J. Crawford[1], M. D. Filipović[1], A. Y. De Horta[1], F. H. Stootman[1] and J. L. Payne[2]

[1]*School of Computing and Mathematics, University of Western Sydney Locked Bag 1797, Penrith South DC, NSW 1797, Australia*

E–mail: *e.crawford@uws.edu.au*

[2]*Centre for Astronomy, James Cook University Townsville, QLD 4811, Australia*

УДК 524.354–77 : 524.722.3
Оригинални научни рад

У овој студији представљамо нове ATCA радио-континум резултате високе резулуције посматрања остатка супернове у Великом Магелановом Облаку – SNR J0455–6838. Нашли смо да овај остатак супернове има типичну морфологију за ову врсту објеката са радио-спектралним индексом од α =–0.81±0.18 и дијаметром од D= 43×31±1 парсека. Детектовали смо у просеку висок ниво поларизације, укључујући неочекивано снажну поларизацију (∼70%) у тзв. региону пробоја материје (breakout region) који се налази северно од центра остатка супернове. Ово је прва детекција овакво снажне поларизације код остатака супернових са регионима пробоја материје.